

## Supporting Information

### Addressing voltage hysteresis in Li-rich cathode materials via gas-solid interface modification

Qing Zhao,<sup>a</sup> Mengke Zhang,<sup>a</sup> Zhengcheng Ye,<sup>a</sup> Yao Li,<sup>a</sup> Lang Qiu,<sup>a</sup> Zhuo Zheng,<sup>b</sup> Yang Liu,<sup>c</sup> Benhe Zhong,<sup>a</sup> Yang Song,<sup>a,\*</sup> Xiaodong Guo<sup>a</sup>

*a College of Chemical Engineering, Sichuan University, Chengdu 610065, Sichuan, China.*

*b The State Key Laboratory of Polymer Materials Engineering, Polymer Research Institute of Sichuan University, Chengdu 610065, Sichuan, China.*

*c School of Materials Science and Engineering, Henan Normal University, Xinxiang 453007, Henan, China.*

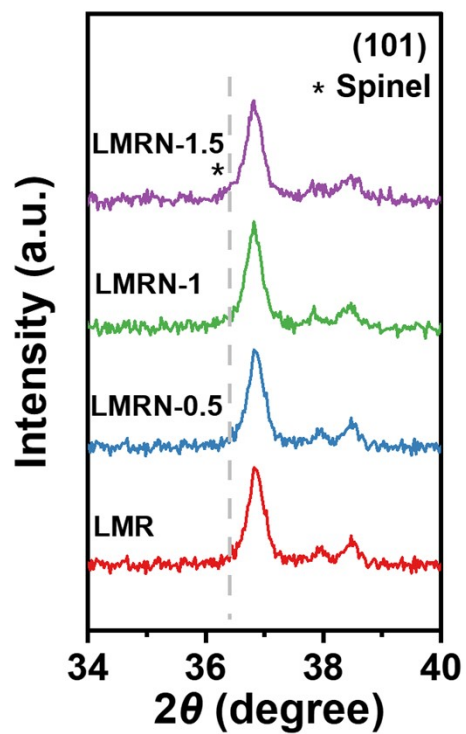
\* Corresponding authors. E-mail addresses: [songyang@scu.edu.cn](mailto:songyang@scu.edu.cn) (Yang Song).

## Supplementary Note 1

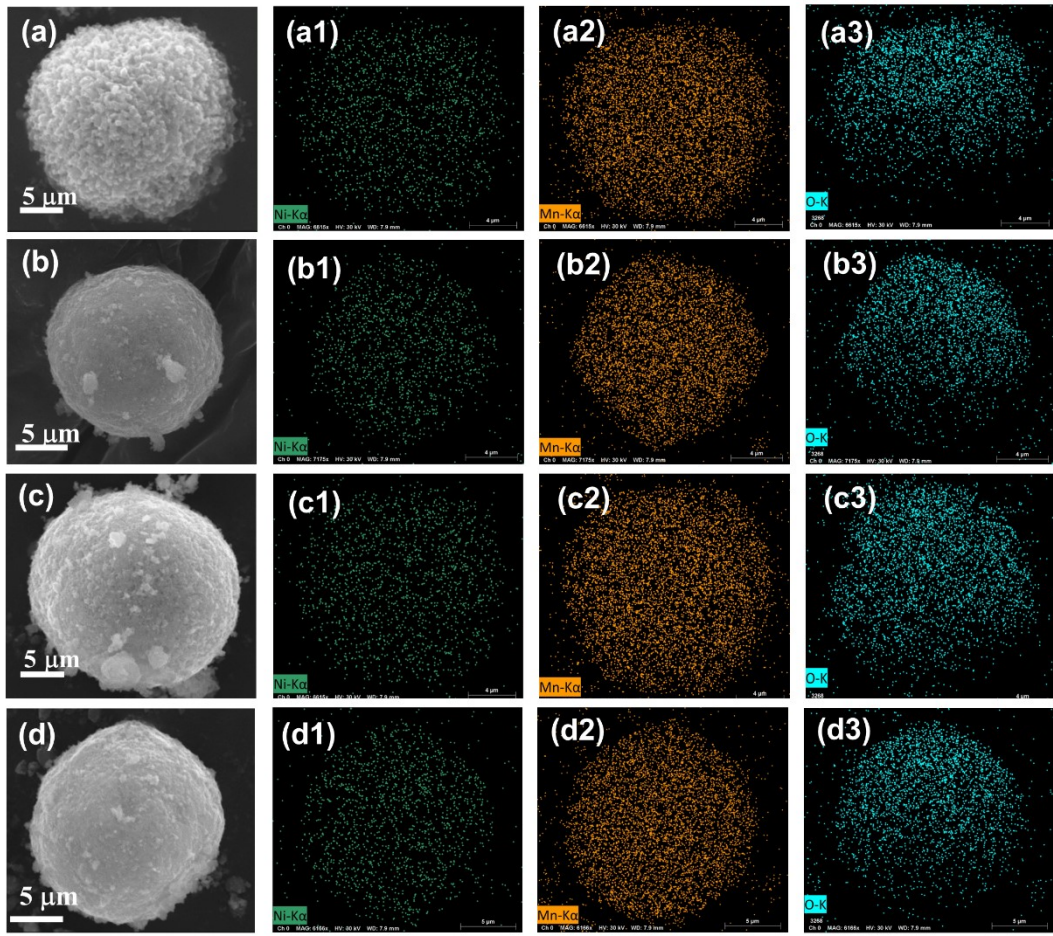
The Calculation Method of Diffusion Coefficient: Li<sup>+</sup> diffusion coefficient ( $D_{Li^+}$ ) is calculated by the following equation:

$$D_{Li^+} = \frac{4}{\pi\tau} \left( \frac{m_B V_m}{M_B S} \right)^2 \left( \frac{\Delta E_s}{\Delta E_\tau} \right)^2$$

In this formula,  $\tau$ ,  $m_B$ ,  $M_B$ , and  $V_m$  respectively stand for the time duration during the current pulse, active material mass on the electrode, molecular weight, and molar volume of active material.  $S$  means the contact area between the electrolyte and the electrode.  $\Delta E_s$  is the steady-state voltage change, and  $\Delta E_\tau$  is the potential change during charging or discharging at the time of current of flux after subtracting the IR drop.<sup>1</sup>

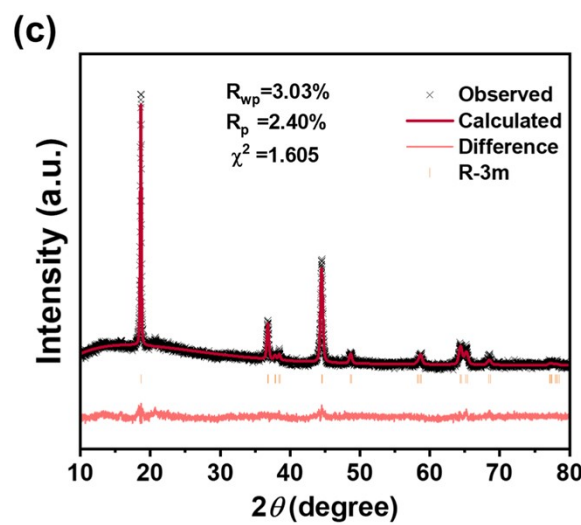
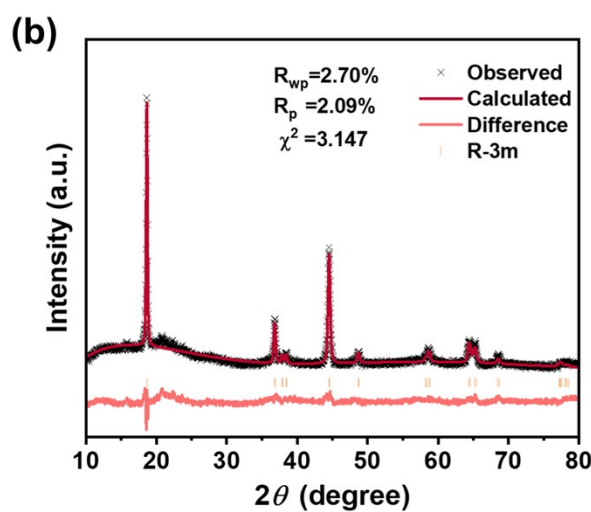
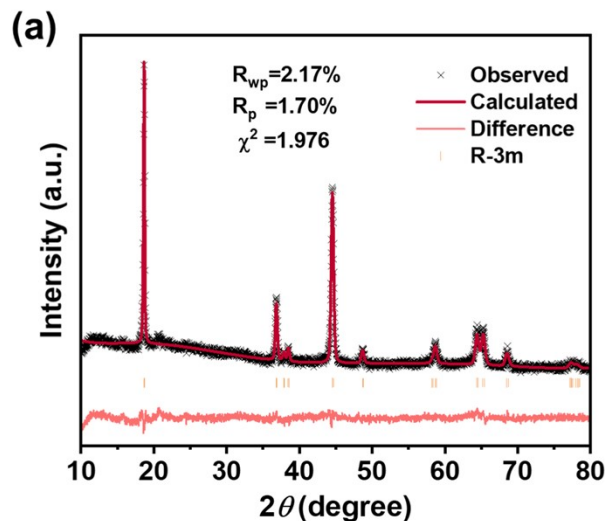


**Fig. S1** The enlargement views of the diffraction peaks of (101).



**Fig. S2** The SEM and EDS-mapping images of pristine and modified samples: (a) LMR, (b) LMRN-0.5, (c) LMRN-1 and (d) LMRN-1.5; the EDS-mapping images of (a1-a3) LMR, (b1-b3) LMRN-0.5, (c1-c3) LMRN-1 and (d1-d3) LMRN-1.5.

EDS mapping is carried out to reveal the elemental dispersion of selected areas, where elemental Mn (yellow), Ni (green), and O (blue) of the target materials are uniformly distributed, suggesting the oxygen vacancy uniform generated does not affect the distribution of the elements.



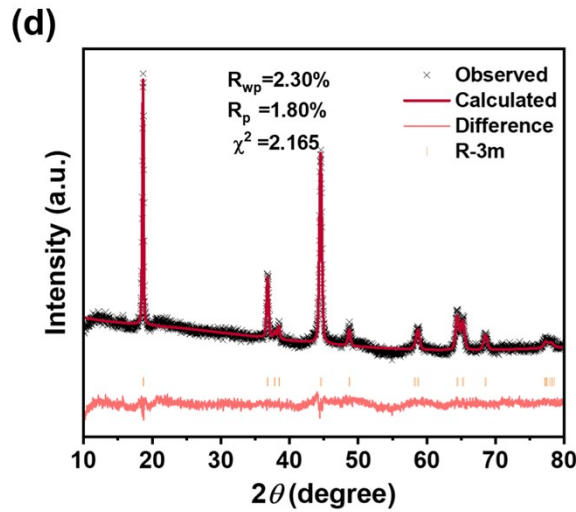


**Fig. S3** XRD Rietveld refinements of (a) LMR, (b) LMRN-0.5, (c) LMRN-1, (d) and LMRN-1.5.

Fig. S3 shows the Rietveld refinements of all materials respectively. It can be seen that  $R_{wp}$  and  $R_p$  in all the Rietveld refinements data are less than 10%, indicating that the results are more accurate.

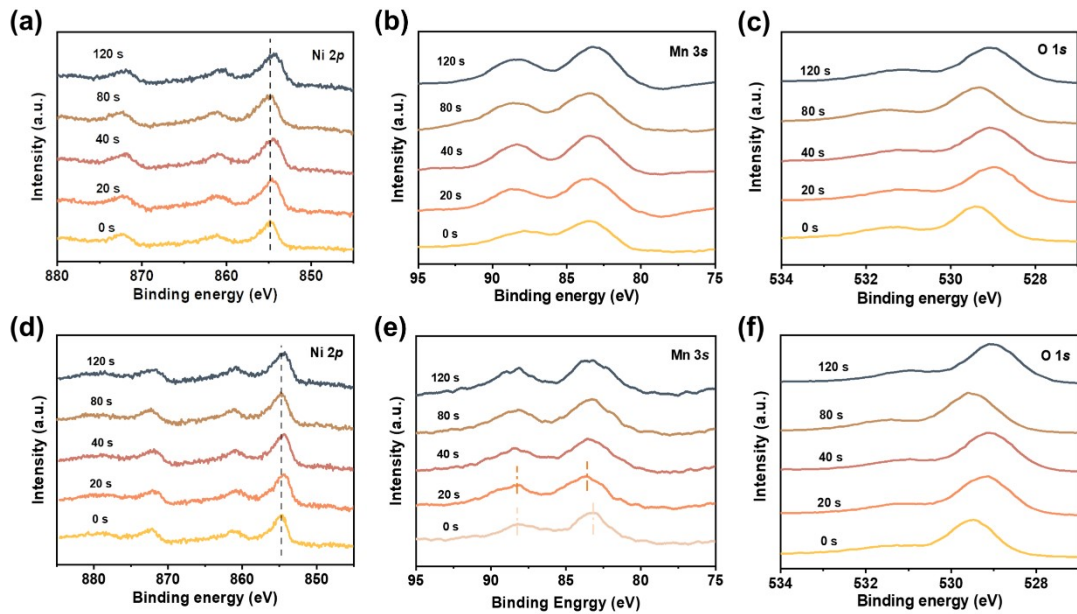


**Fig. S4** XPS profiles of (a) Ni 2p, (b) Mn 3s, and (c) O 1s of LMR and (d) Ni 2p, (e) Mn 3s, and (f) O 1s of LMRN-1 at various depths.

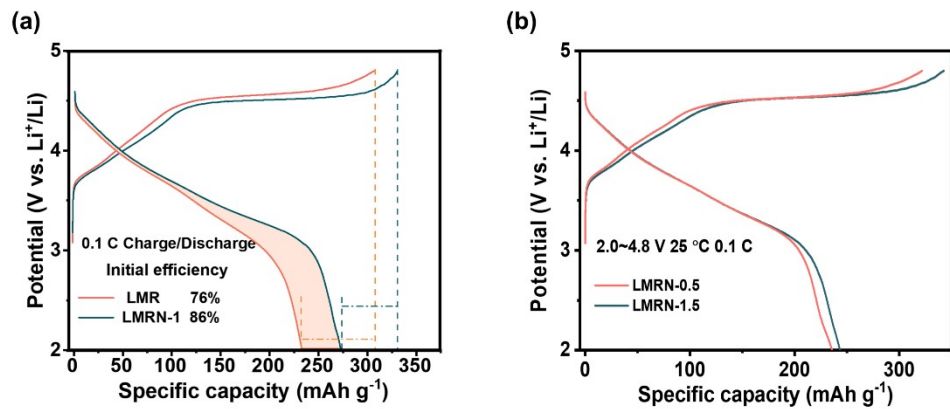


**Fig. S5** (a) Initial charge/discharge curves of LMR and LMRN-1 sample and (b) The initial charge and discharge curves of other samples at 0.1 C, 25 °C, and 2.0-4.8 V.

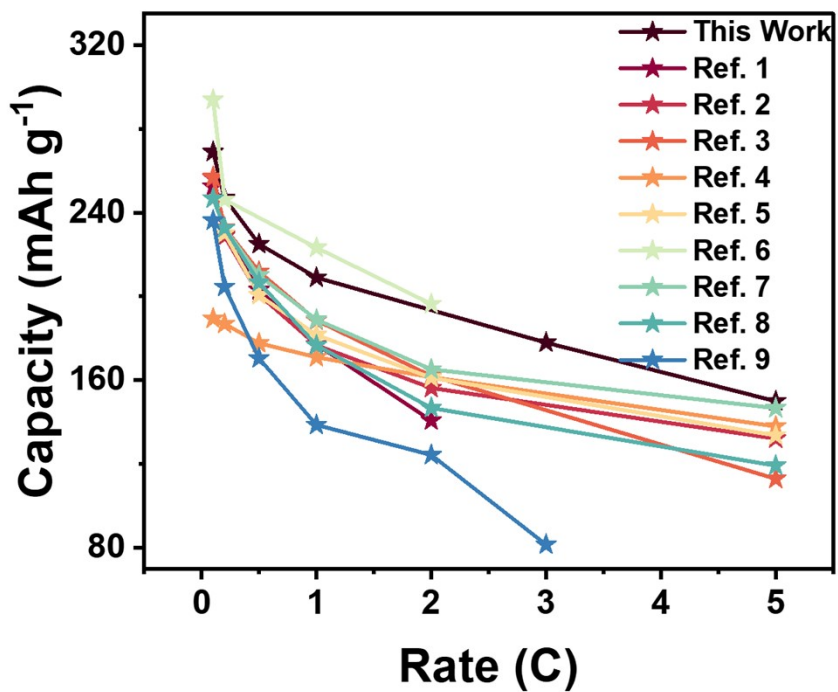


**Fig. S6** Comparison of discharge capacity at different current densities between this work and previous reports.<sup>3-11</sup>

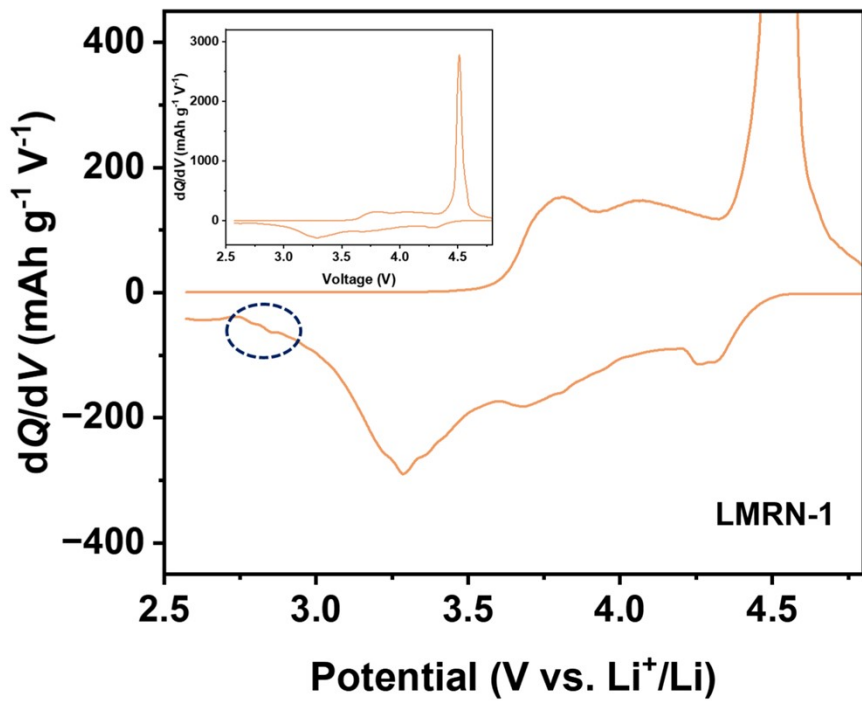


**Fig. S7** Differential capacity ( $dQ/dV$ ) plots versus voltage of first cycle of electrodes prepared from LMRN-1 at 0.1 C.

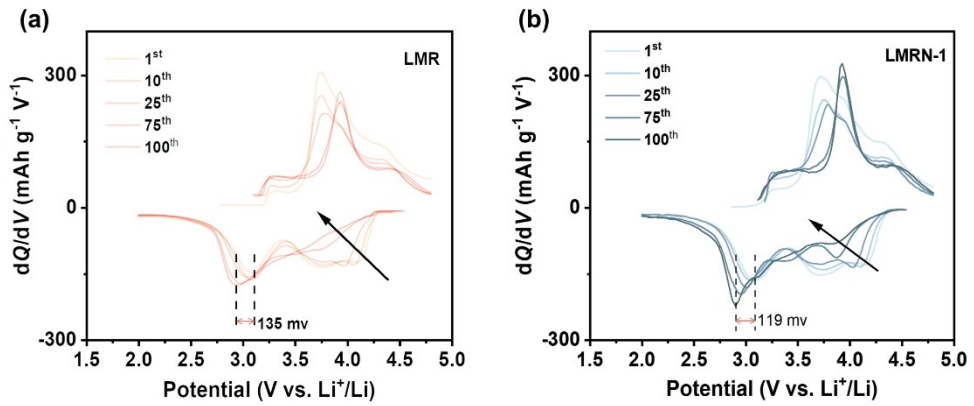


**Fig. S8** Differential charge capacity curves of (a) LMR and (b) LMRN-1 in 100 cycles between 2.0 and 4.8 V.

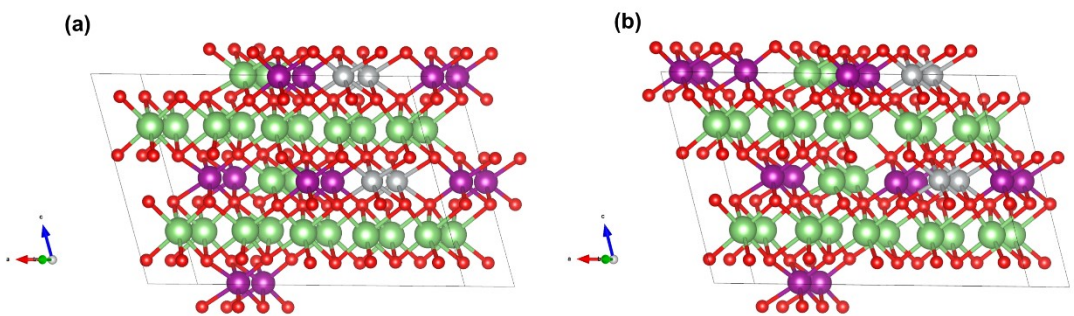


**Fig. S9** The crystal structure model of (a) pristine and (b) LMRN-1 sample for DFT calculation.

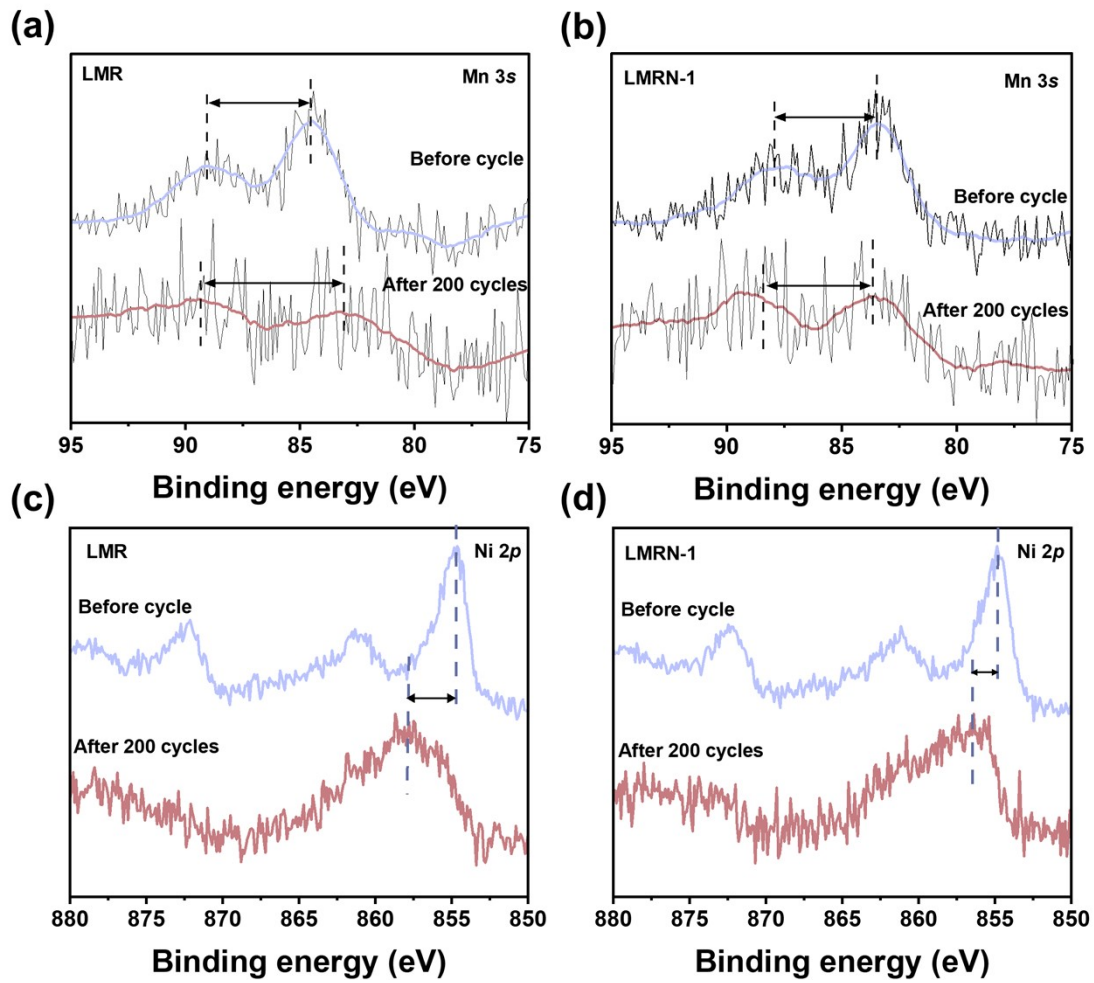


**Fig. S10** The XPS spectra of Mn 3s and Ni 2p for LMR (a and c), LMRN-1 (b and d) before cycle and after 200 cycles.

**Table S1.** The Rietveld refinement for LMR, LMRN-0.5, LMRN-1.0 and LMRN-1.5.

Material	$a$ (Å)	$c$ (Å)	$c/a$
LMR	2.8586	14.2525	4.9858
LMRN-0.5	2.8598	14.2527	4.9838
LMRN-1.0	2.8666	14.2782	4.9810
LMRN-1.5	2.8610	14.2534	4.9819

**Table S2.** Comparison of discharge capacity at different current densities between this work and previous reports.

Cathode	0.1C	0.2C	0.5C	1C	2C	3C	5 C	Cycle performance	Ref.
$\text{Li}_{1.2}\text{Ni}_{0.2}\text{Mn}_{0.6}\text{O}_2$	269.0	247.0	225.0	209.0		178.0	150.0	1 C-200 cycles-90%	This work
$\text{Li}_{1.2}\text{Ni}_{0.2}\text{Mn}_{0.6}\text{O}_2$	252.4	229.5	203.0	177.1	140.8			0.5 C-300 cycles-80%	3
$\text{Li}_{1.2}\text{Ni}_{0.2}\text{Mn}_{0.6}\text{O}_2$	256.6	228.7	200.8	176.7	156.3		132.1	0.1 C-100 cycles-93%	4
$\text{Li}_{1.2}\text{Mn}_{0.54}\text{Ni}_{0.13}\text{Co}_{0.13}\text{O}_2$	257.0	232.8	211.9	188.5	162.0		112.9	2 C-700 cycles-81%	5
$\text{LiNi}_{0.6}\text{Mn}_{0.2}\text{Co}_{0.2}\text{O}_2$	189.4	186.9	177.7	170.9	161.4		137.9	1 C-150 cycles-98%	6
$\text{Li}_{1.2}\text{Ni}_{0.2}\text{Mn}_{0.6}\text{O}_2$		230.1	200.6	181.7	161.2		133.7	1 C-100 cycles-80%	7
$\text{Li}_{1.2}\text{Mn}_{0.54}\text{Ni}_{0.13}\text{Co}_{0.13}\text{O}_2$	293.9		246.2	223.2	196.4			0.1 C-100 cycles-95%	8
$\text{Li}_{1.2}\text{Ni}_{0.2}\text{Mn}_{0.6}\text{O}_2$		223.5	210.1	188.9	165.2		146.7	1 C-500 cycles-86%	9
$\text{Li}_{1.2}\text{Mn}_{0.56}\text{Ni}_{0.16}\text{Co}_{0.08}\text{O}_2$	246.8	232.6	206.7	176.7	146.7		119.3	1 C-500 cycles-87%	10
$\text{Li}_{1.7}\text{Mn}_{0.8}\text{Co}_{0.1}\text{Ni}_{0.1}\text{O}_{2.7}$	236.2	204.6	170.4	138.6	124.3	81.5		0.2 C-500 cycles-76%	11

**Table S3.** The EIS fitting results for the LMR, LMRN-0.5, LMRN-1.0 and LMRN-1.5 materials.

Material	Before the cycle		After 200 cycles	
	Re ( $\Omega$ )	Rct ( $\Omega$ )	Re ( $\Omega$ )	Rct ( $\Omega$ )
LMR	1.414	89.04	9.593	137.3
LMRN-0.5	1.815	65.00	3.606	109.4
LMRN-1.0	1.083	34.40	12.70	46.70
LMRN-1.5	2.898	71.15	4.527	103.8

## References

- 1 B. Xiao, Y. Wang, S. Tan, M. Song, X. Li, Y. Zhang, F. Lin, K. S. Han, F. Omenya, K. Amine, X. Q. Yang, D. Reed, Y. Hu, G. L. Xu, E. Hu, X. Li and X. Li, *Angew. Chem. Int. Ed.*, 2021, **60**, 8258-8267.
- 2 S. Jeong, K. Choi, V. C. Ho, J. Cho, J. S. Bae, S. C. Nam, T. Yim and J. Mun, *Chem. Eng. J.*, 2022, **434**, 1314577.
- 3 W. Zhu, Z. G. Tai, C. Y. Shu, S. K. Chong, S. W. Guo, L. J. Ji, Y. Z. Chen and Y. N. Liu, *J. Mater. Chem. A*, 2020, **8**, 7991-8001.
- 4 S. Zhao, B. Sun, K. Yan, J. Zhang, C. Wang and G. Wang, *ACS Appl. Mater. Interfaces*, 2018, **10**, 33260-33268.
- 5 W. Zhang, Y. Sun, H. Deng, J. Ma, Y. Zeng, Z. Zhu, Z. Lv, H. Xia, X. Ge, S. Cao, Y. Xiao, S. Xi, Y. Du, A. Cao and X. Chen, *Adv. Mater.*, 2020, **32**, e2000496.
- 6 W. Bao, G. Qian, L. Zhao, Y. Yu, L. Su, X. Cai, H. Zhao, Y. Zuo, Y. Zhang, H. Li, Z. Peng, L. Li and J. Xie, *Nano Lett.*, 2020, **20**, 8832-8840.
- 7 S. Chen, Y. Zheng, Y. Lu, Y. Su, L. Bao, N. Li, Y. Li, J. Wang, R. Chen and F. Wu, *ACS Appl. Mater. Interfaces*, 2017, **9**, 8669-8678.
- 8 S. Liu, Z. P. Liu, X. Shen, W. H. Li, Y. R. Gao, M. N. Banis, M. S. Li, K. Chen, L. Zhu, R. C. Yu, Z. X. Wang, X. L. Sun, G. Lu, Q. Y. Kong, X. D. Bai and L. Q. Chen, *Adv. Energy Mater.*, 2018, **8**, 201802105.
- 9 L. Nie, Z. Wang, X. Zhao, S. Chen, Y. He, H. Zhao, T. Gao, Y. Zhang, L. Dong, F. Kim, Y. Yu and W. Liu, *Nano Lett.*, 2021, **21**, 8370-8377.
- 10 J. X. Meng, L. S. Xu, Q. X. Ma, M. Q. Yang, Y. Z. Fang, G. Y. Wan, R. H. Li, J. J. Yuan, X. K. Zhang, H. J. Yu, L. L. Liu and T. F. Liu, *Adv. Funct. Mater.*, 2022, **32**, 2113013.

11 C. Huang, Z. Q. Fang, Z. J. Wang, J. W. Zhao, S. X. Zhao and L. J. Ci, *Nanoscale*, 2021, **13**, 4921-4930.